2．学会発表

なし。

H. 知的所有権の出願・取得状況（予定を含む）

なし。

Ⅲ．研究成果の刊行物・一覧

書籍：なし

雑誌

発表者氏名	論文タイトル	発表誌名	巻	ページ	出版年
Sakudo A., Baba K., Tsukamoto M., Sugimoto A., Okada T., Kobayashi T., Kawashita N., Takagi T., Ikuta K.	Anionic polymer, poly(methyl vinyl ether-maleic anhydride)-coated beads-based capture of human influenza A and B virus	*Bioorg. Med. Chem.*	17	752–757	2009
Hiromatsu K.; Takahara J.; Nishihara T.; Okamoto K.; Yasunaga T.; Ohmayu Y.; Takagi T.; Nakazono K.	Prediction for Biodegradability of Chemicals by Kernel Partial Least Squares	*J. Comput. Aided Chem.*	10	1–9	2009
Kanbayashi, Y.; Okamoto, K.; Ogaru, T.; Hosokawa, T.; Takagi, T.	Statistical validation of the relationships of cancer pain relief with various factors using ordered logistic regression analysis	*Clinical J. Pain*	25	65–72	2009
Kanbayashi Y.; Nomura K.; Fujimoto Y.; Yamashita M.; Ohshiro M.; Okamoto K.; Matsumoto Y.; Horiike S.; Takagi T.; Ishida Y.; Taniwaki M.	Risk factors for infection in haematology patients treated with rituximab	*Eur. J. Haematol.*	82	26–30	2009
Nakamura S., Yang C.-S., Sakon N., Ueda M., Tougan T., Yamashita A., Goto N., Takahashi K., Yasunaga T., Ikuta K., Mizutani T., Okamoto Y., Tagami M., Morita R., Maeda N., Kawai J., Hayashizaki Y., Nagai Y., Horii T., Iida T., Nakaya T.	Direct Metagenomic Detection of Viral Pathogens in Nasal and Fecal Specimens using an Unbiased High-throughput Sequencing Approach	*PLoS ONE*	4	e4219	2009
Nishikawa, H., Nakamura, S., Kodama, E., Ito, S., Kajiwara, K., Izumi, K., Sakagami, Y., Oishi, S., Ohkubo, T., Kobayashi, Y., Otaka, A., Fujii, N.,	Electrostatically constrained alpha-helical peptide inhibits replication of HIV-1 resistant to enfuvirtide	*Int. J. Biochem. Cell. Biol.*	41	891–899	2009

Matsuoka, M.					
Okada N., Iida T., Park K.-S., Goto N., Yasunaga T., Hiyoshi H., Matsuda S., Kodama T., Honda T.	Identification and characterization of a novel type III secretion system in trh-positive Vibrio parahaemolyticus strain TH3996 reveal genetic lineage and diversity of pathogenic machinery beyond the species level.	*Infect. Immun.*	77	904–913	2009
Utachee, P.; Jinnopat, P.; Isarangkura-Na-Ayuthaya, P.; de Silva, U.C.; Nakamura,S.; Siripanyaphinyo, U.; Wichukchinda, N.; Tokunaga, K.; Yasunaga, T.; Sawanpanyalert, P.; Ikuta, K.; Auwanit, W.; Kameoka, M.	Phenotypic studies on recombinant human immunodeficiency virus type 1 (HIV-1) containing CRF01_AE env gene derived from HIV-1-infected patient, residing in central Thailand.	*Microbes Infect.*	11	334-343	2009
Du, A.; Daidoji, T.; Koma, T.; Ibrahim, M.S.; Nakamura, S.; de Silva, U.C.; Ueda, M.; Yang, C.; Yasunaga, T.; Ikuta,K.; Nakaya,T.	Detection of circulating Asian H5N1 viruses by a newly established monoclonal antibody.	*Biochem Biophys Res Commun.*	378	197–202	2009
川下理日人	目指せ！第 2 世代の HIV インテグラーゼ阻害剤	*ファルマシア*	44	1216–1217	2008
Hakamada, S., Sonoyama, T., Ichiki, S., Nakamura, S., Uchiyama, S., Kobayashi, Y., Sambongi, Y.	Stabilization mechanism of cytochrome c552 from a moderately thermophilic bacterium, Hydrogenophilus thermoluteolus	*Biosci. Biotechnol. Biochem*	72	2103–2109	2008
Li, S. M., Li, G. M., Nakamura, S., Ikuta, K., Nakaya, T.	Reduced incorporation of SARS-CoV spike protein into viral particles due to amino acid substitutions within the receptor binding domain	*Jpn J Infect Dis,*	61	123–127	2008
Matsumoto, S., Yoshida, T., Murata, H., Harada, S., Fujita, N., Nakamura, S., Yamamoto, Y., Watanabe, T., Yonekura, H., Yamamoto, H., Ohkubo, T., Kobayashi, Y.	Solution Structure of the Variable-Type Domain of the Receptor for Advanced Glycation End Products: New Insight into AGE-RAGE Interaction	*Biochemistry*	47	12299–12311	2008

Nakamura, S., Maeda, N., Miron, I. M., Yoh, M., Izutsu, K., Kataoka, C., Honda, T., Yasunaga, T., Nakaya, T., Kawai, J., Hayashizaki, Y., Horii, T., and Iida, T.	Metagenomic diagnosis of bacterial infections	*Emerg. Infect. Dis.*	14	1784–1786	2008
Takeuchi M.; Okamoto K.; Takagi T.; Ishii H.	Ethnic difference in inter-East Asian subjects with normal glucose tolerance and impaired glucose regulation: a systematic review and meta-analysis focusing on fasting serum insulin	*Diabetes Res. Clin. Pract.*	82	383–390	2008
Takeuchi M.; Okamoto K.; Takagi T.; Ishii H.	Ethnic difference in patients with type 2 diabetes mellitus in inter-East Asian populations: A systematic review and meta-analysis focusing on fasting serum insulin.	*Diabetes Res. Clin. Pract.*	81	370–376	2008
Kanbayashi, Y.; Nomura, K.; Fujimoto, Y.; Shimura, K.; Shimizu, D.; Okamoto, K.; Matsumoto, Y.; Horiike, S.; Shimazaki, C.; Takagi, T.; Taniwaki, M.	Population Pharmacokinetics of Itraconazole Solution Used as Prophylaxis for Febrile Neutropaenia.	*Int. J. Antimicrobial Agents.*	31	452–457	2008
Ohgaru, T.; Shimizu, R.; Okamoto, K.; Kawase, M.; Shirakuni,Y.; Nishikiori, R.; Takagi, T.	Ordinal Classification Using Comparative Molecular Field Analysis	*J. Chem. Inf. Model.*	48	207–212	2008
Nishikiori R., Yamaguchi M., Takano K., Enatsu T., Tani M., de Silva U. C., Kawashita N., Takagi T., Morimoto S., Hangyo M., Kawase M.	Application of Partial Least Square on Quantitative Analysis of L-, D-, and DL-Tartaric Acid by Terahertz Absorption Spectra.	*Chem. Pharm. Bull.*	56	305–307	2008
Nishikiori R., Makino Y., Ochi Y., Yamashita N., Okamoto K., Kawashita N., Takahara J.-i., Yasunaga T., Takagi T., Kawase M.	Development of Fingerprint Verification Type Self-Organized Map Applied to Profiling Seized Methamphetamine.	*J. Comput. Aided Chem.*	9	30–36	2008
Ohgaru, T., Shimizu, R.,	Enhancement of Ordinal CoMFA	*J. Chem. Inf.*	48	910–917	2008

Okamoto, K., Kawashita, N., Kawase, M., Shirakuni, Y., Nishikiori, R., Takagi, T.	by Ridge Logistic Partial Least Squares	*Model*			
Yamashita A., Goto N., Nishiguchi S., Shimada K., Yamanishi H., Yasunaga T.	Computational search for over-represented 8-mers within the 5'-regulatory regions of 634 mouse testis-specific genes	*Gene*	427	93–98	2008

Ⅳ．研究成果の刊行物・別刷（抜粋）

1．Electrostatically constrained alpha-helical peptide inhibits replication of HIV-1 resistant to enfuvirtide

Nishikawa, H., Nakamura, S., Kodama, E., Ito, S., Kajiwara, K., Izumi, K., Sakagami, Y., Oishi, S., Ohkubo, T., Kobayashi, Y., Otaka, A., Fujii, N., and Matsuoka, M.

Int. J. Biochem. Cell. Biol., **41**, 891-899, (2009).

2．Statistical validation of the relationships of cancer pain relief with various factors using ordered logistic regression analysis

Kanbayashi, Y.; Okamoto, K.; Ogaru, T.; Hosokawa, T.; Takagi, T.

Clinical J. Pain, **25**, 65-72, (2009).

The International Journal of Biochemistry & Cell Biology 41 (2009) 891–899

Contents lists available at ScienceDirect

The International Journal of Biochemistry & Cell Biology

journal homepage: www.elsevier.com/locate/biocel

Electrostatically constrained α-helical peptide inhibits replication of HIV-1 resistant to enfuvirtide

Hiroki Nishikawa[a], Shota Nakamura[b], Eiichi Kodama[c,*], Saori Ito[a], Keiko Kajiwara[c,d], Kazuki Izumi[c], Yasuko Sakagami[c], Shinya Oishi[a], Tadayasu Ohkubo[e], Yuji Kobayashi[f], Akira Otaka[g], Nobutaka Fujii[a], Masao Matsuoka[c]

[a] Graduate School of Pharmaceutical Sciences, Kyoto University, Sakyo-ku, Kyoto 606-8501, Japan
[b] Research Institute for Microbial Diseases, Osaka University, Suita, Osaka 565-0871, Japan
[c] Laboratory of Virus Control, Institute for Virus Research, Kyoto University, Sakyo-ku, Kyoto 606-8507, Japan
[d] Institute for Virus Research, and Graduate School of Biostudies, Kyoto University, Sakyo-ku, Kyoto 606-8507, Japan
[e] Graduate School of Pharmaceutical Sciences, Osaka University, Suita, Osaka 565-0871, Japan
[f] Osaka University of Pharmaceutical Sciences, Takatsuki, Osaka 569-1094, Japan
[g] Graduate School of Pharmaceutical Sciences, The University of Tokushima, Tokushima 770-8505, Japan

ARTICLE INFO

Article history:
Received 7 July 2008
Received in revised form 19 August 2008
Accepted 22 August 2008
Available online 10 September 2008

Keywords:
HIV
Fusion
Peptide
Inhibitor
α-Helix

ABSTRACT

α-Helical peptides, such as T-20 (enfuvirtide) and C34, derived from the gp41 carboxyl-terminal heptad repeat (C-HR) of HIV-1, inhibit membrane fusion of HIV-1 and the target cells. Although T-20 effectively suppresses the replication of multi-drug resistant HIV variants both in vitro and in vivo, prolonged therapy with T-20 induces emergence of T-20 resistant variants. In order to suppress the emergence of such resistant variants, we introduced charged and hydrophilic amino acids, glutamic acid (E) and lysine (K), at the solvent accessible site of C34. In particular, the modified peptide, SC34EK, demonstrates remarkably potent inhibition of membrane fusion by the resistant HIV-1 variants as well as wild-type viruses. The activity was specific to HIV-1 and little influenced by serum components. We found a strong correlation between the anti-HIV-1 activities of these peptides and the thermostabilities of the 6-helix bundles that are formed with these peptides. We also obtained the crystal structure of SC34EK in complex with a 36 amino acid sequence (N36) comprising the amino-terminal heptad repeat of HIV-1. The EK substitutions in the sequence of SC34EK were directed toward the solvent and generated an electrostatic potential, which may result in enhanced α-helicity of the peptide inhibitor. The 6-helix bundle complex of SC34EK with N36 appears to be structurally similar to that of C34 and N36. Our approach to enhancing α-helicity of the peptide inhibitor may enable future design of highly effective and specific HIV-1 inhibitors.

© 2008 Elsevier Ltd. All rights reserved.

1. Introduction

Enfuvirtide (T-20), which has been clinically approved as the first fusion inhibitor of HIV-1, is derived from a 36 amino acid region of the carboxyl-terminal heptad repeat (C-HR) of gp41, an HIV-1 transmembrane envelope glycoprotein, which plays central role in the fusion of HIV-1 with host cells. T-20 prevents the formation of a 6-helix bundle, which is comprised of a trimer of dimers formed from the amino-terminal heptad repeat (N-HR) and the carboxyl-terminal heptad repeat (C-HR) in an antiparallel orientation. Six-helix formation by physiological gp41 enables host cell and virus membranes to contact and fuse, enabling the virus entry into the cells. Therefore, inhibition of the formation of this 6-helix bundle prevents fusion of HIV-1 and targeted host cell membranes (Derdeyn et al., 2000; Wild et al., 1992). Notably, T-20 effectively suppresses the replication of HIV-1 variants, which are resistant to multiple reverse transcriptase and protease inhibitors, and has been used in the optimized regimens for HIV-1-infected patients harboring multi-drug resistant HIV-1 variants (Lalezari et al., 2003; Lazzarin et al., 2003).

Emergence of T-20-resistant HIV-1 was reported not only in patients receiving T-20 monotherapy in a phase I clinical trial (Wei et al., 2002), but also in patients treated with a combination of T-20

* Corresponding author at: 53 Kawaramachi Shogoin, Sakyo-ku, Kyoto 606-8507, Japan. Tel.: +81 75 751 3986; fax: +81 75 751 3986.
E-mail address: ekodama@virus.kyoto-u.ac.jp (E. Kodama).

1357-2725/$ – see front matter © 2008 Elsevier Ltd. All rights reserved.
doi:10.1016/j.biocel.2008.08.039

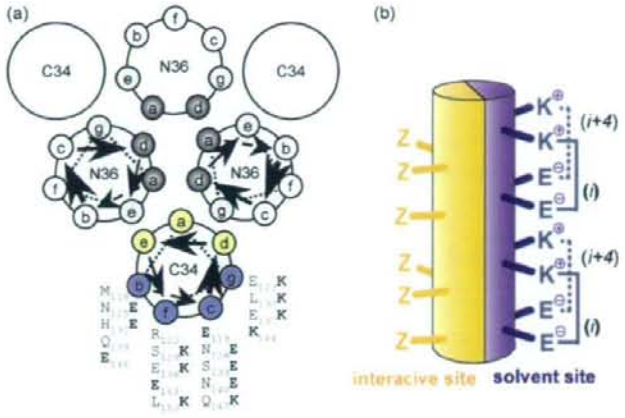

Fig. 1. Helical wheel representation of the 6-helix bundle structure and the design of SC34EK. (a) Amino acid residues at positions a, d, e of C34 are interactive sites that form the 6-helix complex with N36, while the remaining amino acid residues at positions b, c, f, g are solvent accessible sites, which are substituted with Glu (E) or Lys (K) in SC34EK. (b) The design concept of introducing the EK motif to the solvent accessible site. The α-helical C-HR peptide could be divided into interactive (red) and solvent (blue) sites. Z indicates the original amino acids of C34. Only amino acid residues at solvent sites were replaced by E at the *i* position and K at the *i*+4 position.

and other inhibitors in subsequent phases II and III trials (Matthews et al., 2004; Poveda et al., 2002). These resistant variants frequently acquired mutations in gp41, especially in amino acids 36–45 of the N-HR region (Aquaro et al., 2006; Cabrera et al., 2006; Mink et al., 2005; Poveda et al., 2002; Rimsky et al., 1998; Wei et al., 2002) (Fig. 1). Additionally, complementary mutations in the C-HR region, such as S138A mutation, were found in some T-20 resistant variants (Cabrera et al., 2006; Poveda et al., 2004; Xu et al., 2005). Introduction of these complementary mutations compensates for impaired HIV-1 replication stemming from the primary mutations that give rise to resistance. The N43D mutation in the N-HR region that confers resistance to T-20 is a well documented example (Xu et al., 2005).

Although T-20 inhibits gp41-mediated fusion (Derdeyn et al., 2000; Wild et al., 1992), it has additional effects on HIV-1 replication. For instance, baseline sensitivity of HIV-1 to T-20 is influenced not only by the amino acid sequence of gp41, but also by the co-receptor specificity (CCR5/CXCR4) defined by the structure of the V3 loop of gp120, a glycoprotein capping gp41, which binds to the CD4 cells (Derdeyn et al., 2000; Derdeyn et al., 2001). Moreover, substitutions within the CD4 binding domain of gp120 also contribute to the resistance of the virus to T-20 (Baldwin and Berkhout, 2006). Thus, the mode of action and the mechanism of resistance to T-20 seem to be complicated. In contrast, another fusion inhibitor known as C34, has been clearly shown to bind to the N-HR in vitro and act as a decoy of gp41 C-HR and prevent the formation of the 6-helix bundle (Chan et al., 1997; Liu et al., 2005; Xu et al., 2007). Its inhibitory effect is over 10-fold greater than that of T-20 (Armand-Ugon et al., 2003; Nameki et al., 2005). Thus, C34 appears to be a suitable peptide to employ in the rational design of an improved HIV fusion inhibitor, based on the interaction between the peptide and the target.

It has been reported that α-helicity of the C-HR and N-HR peptide complexes correlates with the anti-HIV-1 activity of the peptide inhibitor (Chan et al., 1998), suggesting that enhancement of α-helicity of C34 may provide higher affinity to the N-HR region, thus resulting in more potent anti-HIV-1 activity. To design potent fusion inhibitors using the enhancement of α-helicity approach, we divided the α-helical peptide C34 into two characteristic interactive (a, d, e) and solvent accessible (b, c, f, g) sites according to the reported N36/C34 structure (Fig. 1) (Chan et al., 1997). When HIV-1 gp41 is folded, a tryptophan-rich domain (WRD) in the N-terminus of C-HR plays an important role in tight and specific binding, through the interaction of the hydrophobic aromatic ring with a deep groove formed by the N-HR coiled coil (Chan and Kim, 1998; Salzwedel et al., 1999). In fact, C34 contains the N-terminal WRD, which binds to a hydrophobic pocket formed by the amino acid residues L57, W60 and K63 on the N-HR trimer surface (Chan et al., 1998; Ferrer et al., 1999), resulting in higher anti-HIV-1 activity of C34 compared to T-20, which lacks the N-terminal WRD. On the other hand, the solvent accessible site appears to contribute little to the formation of the 6-helix bundles, as demonstrated by the crystal structure of C34 bound to N36 (Chan et al., 1997). Therefore, amino acids in the interactive site are indispensable for binding, whereas those in the solvent accessible site may be replaceable (Fig. 1). To enhance the α-helicity of C34, we introduced a series of systematic replacements of amino acid residues in the solvent accessible site, where the original amino acid residues were substituted with charged and hydrophilic glutamic acid (E) or lysine (K) with the intention of forming possible intrahelical salt-bridges (Marqusee and Baldwin, 1987) (Fig. 1b). We obtained two peptides, SC34 and SC34EK (Fig. 2a), both of which gratifyingly demonstrated increased anti-HIV-1 activity (Otaka et al., 2002).

In this study, we demonstrate that SC34EK maintains highly potent activity against T-20 resistant clones of HIV-1, as well as several clinical isolates, and we reveal that the enhanced α-helicity of SC34EK is indeed involved in the improvement of activity. The activities are specific to HIV-1 and are not influenced by serum components. Structural analysis indicates that electrostatic interactions introduced by EK substitutions enhance the conformational stability of the 6-helix bundle, thus preventing HIV-1 fusion with the host cell. The information from our investigations involving the enhanced α-helicity of SC34EK should enable further design of highly effective and specific HIV-1 inhibitors.

2. Materials and methods

2.1. Cells and viruses

MT-2 and 293T cells were grown in RPMI1640- and Dulbecco's modified Eagle medium (DMEM)-based culture medium, respec-

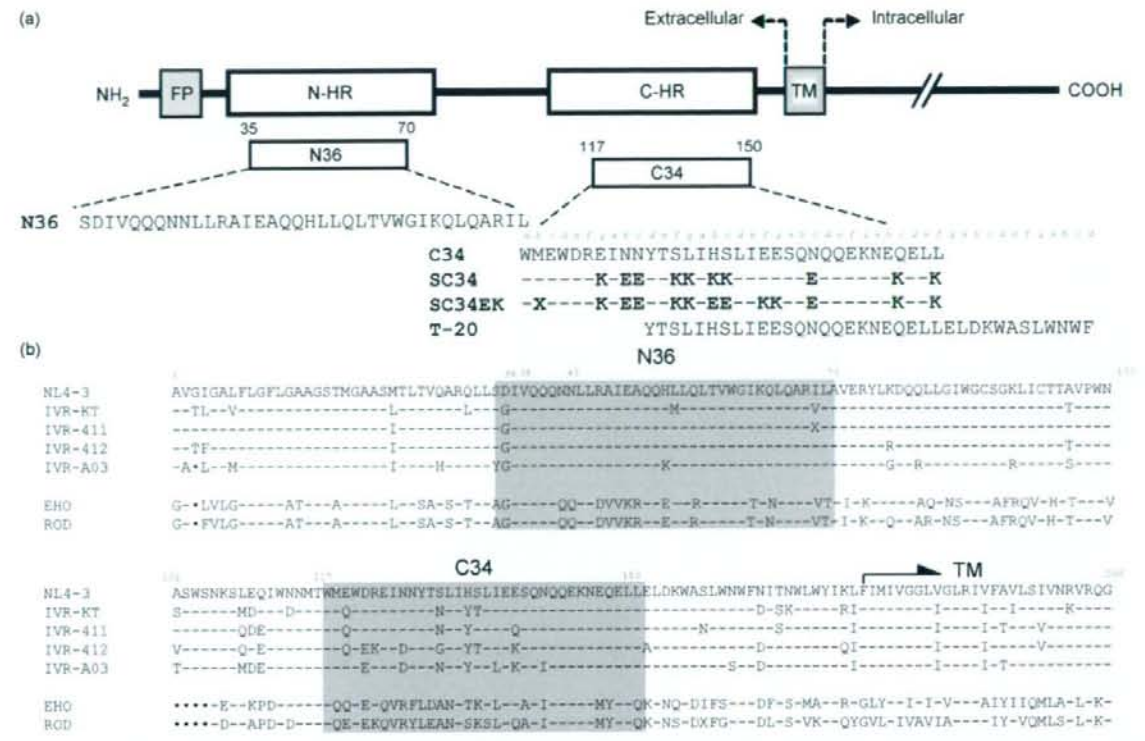

Fig. 2. Schematic view of gp41 and C34 derivatives and amino acid alignment of gp41. (a) The locations of the fusion peptide (FP), the amino-terminal heptad repeat region (N-HR), the carboxyl-terminal heptad repeat region (C-HR), and the transmembrane domain (TM) and the amino acid sequences of N36, T-20, C34 and its derivatives are shown. The residue numbers of each peptide correspond to their positions in gp41 of the NL4-3 strain. The X in SC34EK indicates norleucine, introduced to avoid oxidation of the methionine residues. No differences between the original methionine- and norleucine-containing peptide were observed (Otaka et al., 2002). (b) Alignment of amino acid sequence of clinical isolates (KT, IVR411, IVR412 and IVR-A03; GenBank accession number; AB222704, AB222705, AB222706 and AB222703, respectively) and HIV-2 strains (EHO and ROD) are shown. Corresponding regions of N36 and C34 are indicated in gray. Identical or deleted amino acids from the sequence of NL4-3 are indicated with a bar or a dot, respectively. The X in amino acid sequences of IVR411 and ROD indicates the mixture of I and V for IVR411, and mixture of I and M for ROD.

tively. HeLa-CD4-LTR-β-gal cells were kindly provided by Dr. M. Emerman through the AIDS Research and Reference Reagent Program, Division of AIDS, National Institute of Allergy and Infectious Disease (NIAID) (Bethesda, MD) and were used for the drug susceptibility assay (MAGI assay) as described previously (Kimpton and Emerman, 1992; Kodama et al., 2001; Maeda et al., 1998). The activity of test compounds was determined as the concentration that blocked HIV-1 replication by 50% (EC_{50}).

Laboratory HIV-1 (III_B) and HIV-2 (EHO and ROD) strains were used. An HIV-1 infectious clone pNL4-3 was used for constructions and for the production of HIV-1 variants as described (Nameki et al., 2005). A wild-type HIV-1, HIV-1_{WT}, was generated by transfection of pNL4-3 into 293T cells. Clinical isolates obtained from drug-naïve and heavily drug-experienced patients, were kindly provided by Dr. S. Oka (AIDS Clinical Center, International Medical Center of Japan, Tokyo, Japan). Their co-receptor tropisms were determined using NCK45 cells as described previously (Kajiwara et al., 2006).

2.2. Antiviral agent

The peptide-based fusion inhibitors used in this study were synthesized as described previously (Otaka et al., 2002), and the sequences can be identified in Fig. 2a. 3′-Azido-3′-deoxythymidine (AZT) and 2′,3′-dideoxycytidine (ddC) were purchased from Sigma (St. Louis, MO, USA). MKC-442 was provided by Dr. S. Shigeta (Fukushima Medical University, Fukushima, Japan).

2.3. Determination of drug susceptibility of HIV-1

The peptide sensitivity of infectious clones was determined using the MAGI assay with as described previously (Kodama et al., 2001; Maeda et al., 1998). The activity of test compounds was determined as the concentration that blocks HIV-1 replication by 50% (EC_{50}). For clinical isolates, PHA-stimulated peripheral blood mononuclear cells (PBMCs) were used as described previously (Kodama et al., 2001). PBMCs (10^6 cells/ml) were exposed to test compounds and HIV-1, and were cultured in the presence of interleukin 2 for 7 days. Amounts of p24 protein in the supernatants of the cultures were then determined using the commercially available p24 antigen enzyme linked solvent assay kit.

2.4. Construction of recombinant HIV-1 clone

Recombinant infectious HIV-1 clones with substituted V3 regions, pNL-$V3_{ADA}$ and pNL-$V3_{SF162}$ were generated using pNL4-3. The V3 region, corresponding to n.t. 7029–7249 of pNL4-3, was amplified using primers containing appropriate BglII and NheI restriction enzyme cleavage sites for directional cloning into pBS-

Table 1
Antiviral activity of gp41-derived peptides against gp41 and gp120 V3 recombinant virus[a]

Clone	Tropism[b]	EC_{50} (nM)					
		ddC	N36	T-20	C34	SC34	SC34EK
gp41 recombinant virus							
WT[c]		404 ± 196	180 ± 70	35 ± 17	3.2 ± 0.9	1.4 ± 0.7	0.7 ± 0.3
L33S		289 ± 24	39 ± 11	**>1000**	2.9 ± 0.9	1.3 ± 0.1	0.9 ± 0.3
V38A		714 ± 109	407 ± 76	**402 ± 68**	**96 ± 29**	2.0 ± 0.5	1.1 ± 0.6
V38E		291 ± 57	41 ± 14	**>1000**	**492 ± 85**	**37 ± 12**	**4.3 ± 1.3**
N43K		321 ± 8.5	234 ± 63	114 ± 19	**50 ± 9.5**	2.5 ± 0.3	2.7 ± 0.3
N43D		430 ± 42	461 ± 266	**>1000**	**>100**	**9.0 ± 6.6**	1.0 ± 0.8
D36S/V38M		296 ± 88	178 ± 31	42 ± 6.4	7.2 ± 4.0	1.9 ± 0.1	0.8 ± 0.3
V38E/N42S		273 ± 105	227 ± 20	**>1000**	**322 ± 7.5**	**32 ± 3.1**	3.2 ± 1.0
ΔFNSTW/L33S/N43K[d]		276 ± 39	152 ± 31	**>1000**	**248 ± 56**	2.7 ± 0.3	**4.4 ± 0.5**
ΔFNSTW/D36G/I37K/N126K/L204I[d]		246 ± 67	547 ± 7.8	**754 ± 174**	**67 ± 21**	4.6 ± 0.9	2.9 ± 0.8
gp120 V3 recombinant virus							
V3-ADA	R5	362 ± 102	360 ± 91	**289 ± 19**	6.8 ± 3.3	0.7 ± 0.4	2.0 ± 0.2
V3-SF162[e]	R5	995 ± 219	383 ± 9.9	19 ± 2.8	7.8 ± 3.5	0.5 ± 0.2	0.5 ± 0.2
V3-CH1[f]	R5X4	649 ± 4.5	**2207 ± 42**	16 ± 1	5.6 ± 0.1	1.3 ± 0.1	0.7 ± 0.1
V3-CH2[g]	R5	1515 ± 177	192 ± 13	35 ± 32	3.8 ± 0.1	0.4 ± 0	0.9 ± 0.8

[a] Anti-HIV-1 activity was determined using the MAGI assay. All data represent means ± standard deviation obtained from the results of three independent experiments. Bold indicates over 5-fold increase in EC_{50} value compared to HIV-1_{WT}.

[b] The co-receptor tropism was determined using NCK45 cells as described (Kajiwara et al., 2006).

[c] HIV-1_{NL4-3} served as a wild-type virus.

[d] ΔFNSTW is the deletion of five amino acids at position 364–368 in the gp120 V4 region of HIV-1_{NL4-3} (Nameki et al., 2005). Fusion inhibitor resistant variants used have been previously reported (Armand-Ugon et al., 2003; Nameki et al., 2005).

[e] The V3 region of NL4-3 gp120 was replaced with the corresponding region of HIV-1_{SF162}.

[f] HIV-$1_{V3\text{-}CH1}$ has mutations in the gp120 V3 region of primary isolate HIV-1_{KMT}, where GKI is substituted by GEI.

[g] HIV-$1_{V3\text{-}CH2}$ has mutation in the gp120 V3 region of the primary isolate HIV-1_{KMT}, where GKI is substituted by GQI.

$gp120_{WT}$. The resulting amplified V3 region was subjected to BglII and NheI digestion, subcloned into pBS-$gp120_{WT}$ containing the corresponding region in the DNA fragment of EcoRI–NheI (1510 bp containing gp120 V1, V2 and V3, n.t. 5740–7249 of pNL4-3) and subsequently ligated into pNL4-3. pNL-$V3_{CH1}$ and $V3_{CH2}$, CCR5 and dual (CXCR4 and CCR5) tropic molecular clones, were kindly donated by Dr. Y. Maeda, Kumamoto University (Kumamoto, Japan) (Foda et al., 2001; Maeda et al., 2000).

Recombinant infectious HIV-1 clones carrying various mutations in gp120 and/or gp41 were also generated using pNL4-3. Briefly, the desired mutations were introduced using site directed mutagenesis into the region of pSL-$gp41_{WT}$ flanked by the NheI–BamHI restriction enzyme sites (1220 bp containing gp120 V4, V5 and gp41 ectodomain n.t. 7250–8469 of pNL4-3) (Weiner et al., 1994). After restriction enzyme digestion and purification the NheI–BamHI fragments were ligated into pNL4-3, generating a series of molecular clones with the desired mutations.

Each molecular clone was transfected into 293T cells (10^5 cells/6-well culture plate). After 48 h, MT-2 cells (10^6 cells/well) were added and co-cultured with the 293T cells for an additional 24 h. When an extensive cytopathic effect was observed, the supernatants were harvested and stored at −80 °C for further use.

Table 2
Antiviral activity of gp41-derived peptides against clinical isolates[a]

Strain	EC_{50} (nM)				
	AZT	T-20	C34	SC34	SC34EK
NL4-3 (WT)[b]	2.0	36	3.2	0.36	0.4
KT (WT)[b]	2.0	11	0.2	0.1	0.03
IVR411	**7600**	4.1	0.2	3.1	0.04
IVR412	**9060**	23	7.2	**4.8**	0.1
IVR-A03	**1200**	7.0	**17**	**4.1**	0.7

[a] Anti-HIV-1 activity was determined using the amounts of p24 protein in the supernatants of the PHA-stimulated PBMC cultures using commercially available ELISA kit (Kodama et al., 2001). Bold indicates over 5-fold increase in EC_{50} value compared to HIV-1_{WT}.

[b] HIV-1_{NL4-3} and HIV-1_{KT} served as controls.

2.5. Determination of gp41 amino acid sequence

Nucleotide sequences of the clinical isolates were determined using an automated sequencer. Briefly, DNA was extracted from PBMCs infected with the clinical isolates, subjected to nested PCR for the gp41 coding region, and then directly sequenced as described previously (Nameki et al., 2005).

2.6. Measurement of circular dichroism (CD) spectra

N-HR peptides (N36, $N36_{V38A}$ or $N36_{N43D}$) and C-HR peptides (C34 or SC34EK) were incubated at 37 °C for 30 min (the final concentration of both the N-HR peptide and the C-HR peptide were 10 μM in pH 7.4, 12 mM phosphate-buffered solution containing 50 mM NaCl). The wavelength-dependence of molar ellipticity [θ] was monitored at 25 °C as the average of eight scans, and the thermal stability was estimated by monitoring the change in the CD signal at 222 nm in a spectropolarimeter (Model J-710; Jasco, Tokyo, Japan) equipped with a thermoelectric temperature controller. The midpoint of thermal unfolding transition (melting temperature [T_m]) of each complex was determined as described previously (Otaka et al., 2002). The percentages of a-helicity in 6-helix complexes were calculated by comparing the CD signal at 222 nm of N36/C34 or N36/SC34EK complexes in a spectropolarimeter.

2.7. Crystallization, data collection and refinement

Samples for crystallization were prepared by mixing solutions of N36 and SC34EK dissolved in 10 mM sodium acetate buffer at a concentration of 10 mg/mL. The mixture was incubated for 30 min at 37 °C, then was passed through a 22 μm filter. Crystallization was performed by the hanging drop vapor diffusion method at 4 °C. Droplets were prepared of equal amounts (2 μL) of reservoir solution and the peptide solution. Hexagonal prism crystals were obtained under the following conditions: 100 mM sodium acetate buffer (pH 4.0), 200 mM ammonium sulphate, 14% polyethylene glycol monomethyl ether 2000. After screening of

Table 3
Antiviral activity of HIV-1 gp41-derived peptides against HIV-2[a]

HIV-2 strain	EC_{50} (nM)				
	ddC	T-20	C34	SC34	SC34EK
WT[b]	404 ± 196	35 ± 17	3.2 ± 0.9	1.4 ± 0.7	0.7 ± 0.3
$HIV\text{-}2_{EHO}$[c]	925 ± 188	14 ± 3.0 (×0.4)	**639 ± 87 (×200)**	**68 ± 10 (×49)**	**17 ± 1.2 (×24)**
$HIV\text{-}2_{ROD}$[d]	**1808 ± 927**	**176 ± 68 (×5)**	**>1000 (>×313)**	**251 ± 29 (×179)**	**115 ± 33 (×164)**

[a] Anti-HIV-2 activity was determined using the MAGI assay. All data represent mean ± standard deviation obtained from the results of three independent experiments. Bold indicates over 5-fold increase in EC_{50} value compared to $HIV\text{-}1_{WT}$.

[b] $HIV\text{-}1_{NL4\text{-}3}$ served as a wild-type virus.

[c] $HIV\text{-}2_{EHO}$ was dual-tropic HIV-2.

[d] $HIV\text{-}2_{ROD}$ was T-tropic HIV-2.

various cryo-conditions, the suitable condition was found to be the addition of 35% xylitol to the peptide solution and a slight increase in the amount of the precipitant (*ca* 14.5%). The obtained crystals were easily broken by direct transfer from the crystallization condition to the cryo-condition, but the transfer of the fragile crystals could be accomplished by gradual change in conditions using stepwise increase in the amount (0–35% in five steps) of the cryoprotectant.

Data were collected at a beamline BL38B1 of SPring-8. Collected data were processed using DENZO and SCALEPACK from the HKL2000 package (Otwinowski and Minor, 1997). A molecular replacement solution was found using AMoRe (Navaza, 2001), with a molecular model of the HIV-1 gp41 core structure (PDB code: 1AIK). Model refinements and reconstruction were performed using REFMAC5 (Murshudov et al., 1999) and XtalView (McRee, 1999). The final model was refined at a resolution of 2.1 Å, to a crystallographic *R* value of 0.213 and a free *R* value of 0.238. Detailed data collection and refinement statistics are summarized in Table 1. Atomic coordinates and structural factors have been deposited at the Protein Data Bank (PDB code:2Z2T).

3. Results

3.1. Anti-HIV-1 activity of SC34 and SC34EK

We examined the anti-HIV-1 activity of SC34 and SC34EK against not only $HIV\text{-}1_{WT}$ but also T-20- and/or C34-resistant clones observed in vitro. SC34 and especially SC34EK that has aligned EK modification more effectively suppress HIV-1 infection compared to C34 and T-20 (Table 1). D36S/V38M substitutions in the gp41 region ($HIV\text{-}1_{D36S/V38M}$), and a five amino acid (FNSTW) deletion in the V4 region of gp120 (ΔV4) with L33S/N43K in the gp41 region ($HIV\text{-}1_{\Delta V4/L33S/N43K}$) were isolated in vitro (Fikkert et al., 2002; Rimsky et al., 1998). L33S was also selected during C34-resistant induction in vitro (Armand-Ugon et al., 2003). C34 and its derivatives effectively inhibit entry of these clones into the host cell. In particular, SC34EK maintained strong activity even against V38E containing clones, such as $HIV\text{-}1_{V38E/N42S}$ (Armand-Ugon et al., 2003), which showed cross-resistance to T-20, C34 and SC34. Reduction of activities by SC34 and SC34EK was moderate in $HIV\text{-}1_{\Delta FNSTW/L33S/N43K}$ that showed high level resistance to T-20 and C34. Next, we examined the antiviral activities of C34 derivatives against clones containing major primary mutations V38A and N43D, which are mutations frequently observed in T-20 resistant variants in vivo (Cabrera et al., 2006; Derdeyn et al., 2001; Menzo et al., 2004; Poveda et al., 2004; Poveda et al., 2002; Xu et al., 2005) (Table 1). SC34 reduced its antiviral activities against $HIV\text{-}1_{N43D}$, while SC34EK maintained its potent activity, indicating that when EK is bound with the complementary electrostatic interactions appropriately aligned SC34EK can effectively suppress the infection by various clones resistant to T-20 and C34 both in vitro and in vivo.

We further evaluated activities of SC34 and SC34EK against V3-substituted clones (Table 1). $HIV\text{-}1_{V3\text{-}ADA}$ uses mainly the CCR5 co-receptor for its entry into the host cells and has been reported to moderate T-20 resistance (≈10 fold), compared to the CXCR4 using strain of HIV-1, which shows higher susceptibility to fusion inhibitors (Reeves et al., 2002). As reported, the susceptibility of $HIV\text{-}1_{V3\text{-}ADA}$ to T-20 decreased, however, C34 and its derivatives maintained their activity against the same variant. Interestingly, in our experiments, $HIV\text{-}1_{V3\text{-}SF162}$, $HIV\text{-}1_{V3\text{-}CH1}$ and $HIV\text{-}1_{V3\text{-}CH2}$ also showed comparable susceptibility to T-20. These results indicate that sequence variations in the V3 region do not always correlate with the observed T-20 susceptibility and are not involved in the resistance to C34 and its derivatives.

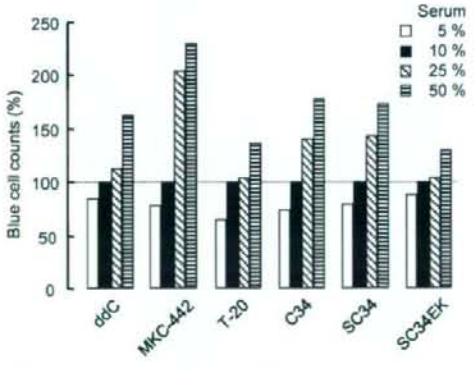

Fig. 3. Effect of FCS concentrations on anti-HIV-1 activity. Changes in the blue cell counts at various concentrations of FCS are shown. Blue cell counts at EC_{50} value in 10% FCS concentration (black bar) were used and set as 100%. White, black, hatched, and striped bars correspond to 5, 10, 25, and 50% FCS, respectively. Inhibitors for reverse transcriptase, ddC and MKC-442, and for fusion, T-20 were used as controls.

3.2. Amino acid sequence

Amino acid sequences of clinical isolates are shown in Fig. 2b. One isolate, $HIV\text{-}1_{KT}$, was obtained from a drug-naïve patient and the other three isolates ($HIV\text{-}1_{411}$, $HIV\text{-}1_{412}$, $HIV\text{-}1_{A03}$) were obtained from heavily drug-experienced patients. None of the patients had received T-20 therapy. Amino acid sequences of the N-HR were highly conserved within all HIV-1 clinical isolates with some small variations. In contrast, the N36 region of the two HIV-2 strains, EHO and ROD, was identical in both HIV-2 isolates. We found some variations in the amino acid sequences of the HIV-2 strains we isolated, as compared with the sequences deposited in the GenBank (accession number; M15390 and X05291 for $HIV\text{-}2_{ROD}$, and U272000 for $HIV\text{-}2_{EHO}$). Namely, we identified two different amino acids in the isolated $HIV\text{-}2_{ROD}$, V26L and

I157I/M (mixture of I and M), and one variation in the amino acid sequence of HIV-2_{EHO}, V45L. Except for I157M, other substitutions are observed in the majority of the HIV-2 strains, as reported in the HIV sequence database (Los Alamos National Laboratory: Los Alamos, NM, USA, http://www.hiv.lanl.gov). These substitutions might be introduced through different culture conditions, (e.g., host cells used for the propagation). We considered these substitutions as a polymorphism.

Sequence homology of the N36 region of the isolated HIV-1 strains was 31/36 (86%), including mutation D36G that is observed in the vast majority of HIV-1 strains (Kuiken et al., 2001). In contrast, those of the C34 region were relatively heterogeneous, 24/34 (71%) for HIV-1 and 12/34 (35%) for HIV-2. Sequence identity of the T-20 region (residues 117–152) in the HIV-1 strains was also variable 27/36 (75%), while in the HIV-2 strains the sequence identity was 15/36 (42%). These results indicate that even highly conserved two helical extracellular domain of the gp41 can allow polymorphisms.

3.3. Efficacy of the peptides against clinical isolates

To evaluate preclinical efficacy, we examined the antiviral activity of C34, SC34 and SC34EK against clinical isolates (Table 2). Replication of HIV-1_{NL4-3} and HIV-1_{KT}, a drug-naïve strain, was suppressed by all compounds tested. C34 showed decreased activity against HIV-$1_{IVR-A03}$, which was isolated from a heavily drug-exposed patient. SC34 also showed reduced susceptibility against three drug-experienced strains. However, it is difficult to conclude whether SC34 showed enhanced susceptibility against HIV-1_{KT} or reduced susceptibility against drug resistant strains. In contrast, T-20 and SC34EK suppressed the replication of all isolates tested to similar extents in EC_{50} values compared to HIV-1_{NL4-3} (Table 2), indicating that SC34EK with appropriately aligned EK residues effectively suppresses the replication of the clinical 3 isolates.

3.4. Anti-HIV-2 activity

To confirm the target specificity, we examined antiviral activities of SC34 and SC34EK against two HIV-2 strains, EHO and ROD. Compared to HIV-1_{NL4-3}, EHO and ROD contain 19 and 22 amino acid substitutions in the C34 region, respectively, and 15 amino acid substitutions in the N36 region, the anticipated site of binding of SC34 and SC34EK peptides (Fig. 2b). Like the parent peptide C34, both SC34 and SC34EK lost their potent activities (Table 3). Compared to HIV-1_{NL4-3}, 6 out of 19 residues in the C34 region of HIV-2_{EHO} and 7 out of 22 residues in the C34 region of HIV-2_{ROD} are located at positions *a*, *d*, and *e* that directly interact with the N36 binding surface. These substitutions in the N36 and C34 region in HIV-2 may be responsible for reduced anti-HIV-2 activities of the peptides derived from HIV-1. At present, we cannot conclude which amino acid substitutions are directly involved in the reduced susceptibility of the HIV-2 strain to the treatment with the peptide fusion inhibitor, and/or whether other regions besides the N36 and C34 regions might influence peptide susceptibility. However, our results indicate that SC34 and SC34EK maintain similar target specificity to the parent peptide, C34.

3.5. Effect of fetal calf serum (FCS) on anti-HIV-1 activity

To estimate the stability of the peptides in vivo, binding level of SC34EK, to serum components, (e.g., albumin) was examined. In this experiment, the antiviral activity in the presence of relatively high concentrations of fetal calf serum (FCS) was determined (Baba et al., 1993) (Fig. 3). EC_{80} values of the fusion inhibitors against HIV-1 replication in vitro were used. In the presence of 50% FCS, the activity of MKC-442 (I-EBU), a lipophilic non-nucleoside RT inhibitor, was reduced 2.3-fold compared with 10% FCS as described previously (Baba et al., 1993). However, the activities of SC34, SC34EK and T-20 were little influenced by serum components. Among the three, SC34EK was the least affected by the concentration of FCS.

We further examined the stability of peptide inhibitors in freshly prepared human sera ($n = 3$). After 1 h incubation of peptides in human sera (final concentration of 200 μM) at 37 °C, the anti-HIV-1 activity was examined using the MAGI assay. Comparable activities of all peptides tested were observed either with or without the incubation (data not shown). These results indicate that hydrophilic SC34EK likely retains its strong anti-HIV-1 activity in vivo, similarly to T-20, because of its low non-specific binding and protease cleavage in serum.

3.6. Peptide binding affinity

To clarify the mechanism of potent anti-HIV-1 activity observed with SC34EK, the binding affinity of SC34EK was evaluated by collecting the CD spectra using synthetic peptides. The CD spectra of equimolar mixtures of the N-HR and C-HR peptides showed spectrum minima at 208 and 222 nm, which indicate the presence of stable α-helical conformations. All combinations of peptides showed similar spectra at 25 °C, indicating that these peptides contained the same α-helicity (Fig. 4a), although the spectrum of C34 with N36 and N43D mutation ($N36_{N43D}$) indicated only weak α-helicity. These results indicate that N43D might reduce the stability of the conformation of the 6-helix bundle, thus decreasing the replication of HIV-1, whereas V38A does not. SC34EK formed stable 6-helix conformations with $N36_{V38A}$ and $N36_{N43D}$. Under these experimental conditions, wavelength-dependent spectra were similar with the exception of the spectrum of the $N36_{N43D}$/C34 complex. Thus, we analyzed thermal stabilities, defined as the midpoint of the thermal unfolding transition (T_m) values, of the potential 6-helix bundles of N-HR and C-HR peptides. T_m of N36/C34 was found to be 52.0 °C, while that of $N36_{V38A}$/C34 and $N36_{N43D}$/C34 decreased to 44.5 and 34.0 °C, respectively (Fig. 3b). In contrast, thermal stabilities of $N36_{V38A}$/SC34EK, $N36_{N43D}$/SC34EK and N36/SC34EK were much higher, 60.5, 56.0 and 69.5 °C, respectively. Thus, binding affinity of SC34EK to N-HR was stronger compared to that of C34. Alternatively, at the physiological temperature of 37 °C, only 60 and 40% of the α-helix content was observed in $N36_{V38A}$/C34 and $N36_{N43D}$/C34 mixtures, respectively, indicating that roughly half of C34 failed to form stably 6-helix bundle with the target N-HR harboring resistant mutations. Therefore, C34 reduces its anti-fusion activity exerted by dominant negative effect. In contrast, only 20% of the unfolded α-helix content was observed in SC34EK with mutated N36, which indicated that at 37 °C, binding of SC34EK to mutated N36 was comparable to that of C34 with wild-type N36 (Fig. 4b). Moreover, physiochemical properties of N-HR and SC34EK complexes, defined by T_m value, correlated well with their ability to inhibit HIV-1 fusion (Fig. 4c). These results suggest that the stability of the 6-helix complex, as judged by the binding stability (affinity), is directly correlated with the anti-HIV-1 activity.

3.7. Crystal structure of the N36/SC34EK complex

The crystal structure of the complex between SC34EK and the N-HR representative peptide N36 was resolved to a resolution of 2.1 Å (Table 4). In the asymmetric unit, a 6-helix bundle consisting of a central helix bundle of three N36 peptides surrounded by three SC34EK peptides was found. This arrangement is similar in the core structure of gp41 (Chan et al., 1997). Structural superimposition of the original gp41 core and the N36/SC34EK complex showed a good match, with an RMSD value of 0.59 for main-chain atoms

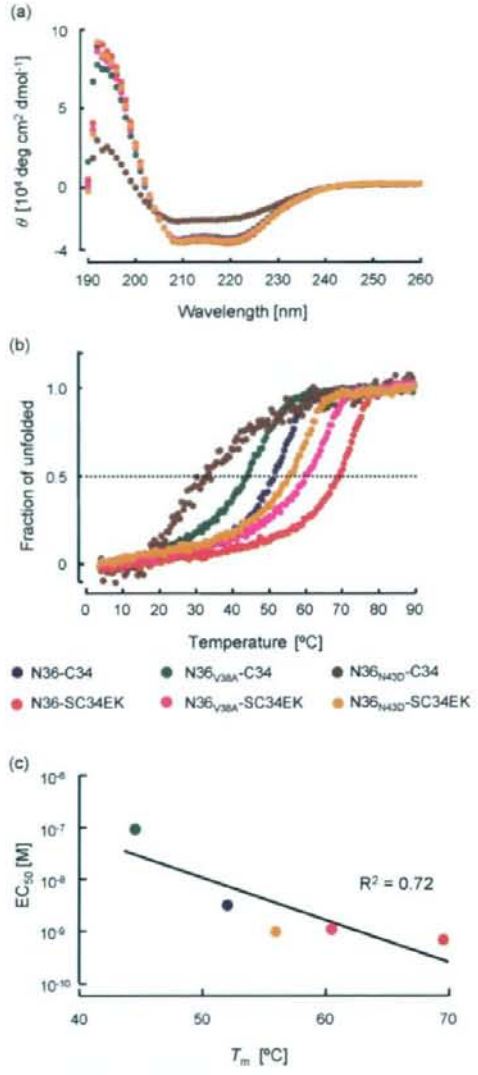

Fig. 4. CD analysis of peptide complex between resistant variants of N36 and C34 or SC34EK. (a) Wavelength-dependent CD spectra of the complexes in solution. The spectrum minima at 208 and 222 nm indicated the presence of stable α-helical conformations. (b) Thermal midpoint analysis was measured at 222 nm CD signal for the N and C peptide complexes. Final concentration of each peptide was 10 mM. The arrow indicates the physiological temperature of 37 °C. (c) The correlation between T_m (b) and EC_{50} values (Table 1). Colors of plots correspond to those in panels (a) and (b). Combination of $N36_{N43D}$ and C34 (EC_{50} > 100 nM) is excluded.

(Fig. 5a and b). Hydrophobic contacts between SC34EK and N36 with tryptophan rich domain (WRD) and leucine zipper were preserved for the original gp41 core. All introduced charged residues of the EK motif were directed toward the solvent (Fig. 5c). As a direct consequence of introducing the EK motifs, the ratio of surface area occupied by charged residues to the total surface area was increased from 35% in the original molecule to 60% in the N36/SC34EK complex. Importantly, it appeared that tight bonding, such as ion pairing or hydrogen bonding, was not present in the

Table 4
Crystallization, data collection and refinement statistics

Data collection	BL38B1 Spring-8
Temperature (K)	100
Space group	$P3_121$
Cell dimensions *a*, *b*, *c* (Å)	105.01, 105.01, 78.31
Resolution limits (Å)	90.00–2.10
Number of unique reflections	29,461
Average redundancy	7.53
Completeness (%)	99.7
R_{merge}[a]	0.122
Refinement statistics	
Refinements resolution range (Å)	20.00–2.20
R/R_{free}[b] (%)	0.213/0.238
The highest resolution shell (Å)	2.15–2.10
R/R_{free}[b] (%)	0.231/0.255
RMSD from ideal	
Bonds (Å)	0.010
Angles (°)	1.015
⟨*B*⟩ for atomic model[c] (Å²)	29.93
Ramachandran plot	
Most favored regions (%)	100

[a] $R_{merge} = \sum|I_h - \langle I_h\rangle|/\sum I_h$, where $\langle I_h\rangle$ is the average intensity of reflection *h* and symmetry-related reflections.
[b] *R* and $R_{free} = \sum||F_o| - |F_c||/\sum|F_o|$ calculated for reflections of the working set and test (5%) set, respectively.
[c] ⟨*B*⟩ is the average temperature factor for all protein atoms.

side-chains of the residues of the EK motif. Electrostatic interaction may involve in constrained structure which provides the enhanced α-helicity observed (Fig. 4). This structural analysis demonstrated that the interaction between N36 and SC34EK retained the ability to form the 6-helix bundle structure despite the substitution of more than one third of the residues (13/34) in the sequence of SC34EK.

4. Discussion

In this study, we characterized a novel α-helical peptide, SC34EK that effectively inhibits replication of HIV-1 strains resistant to T-20 and C34. The activity was specific to HIV-1 and little influenced by serum components. We demonstrate that the potent anti-HIV-1 activity of SC34EK is derived from its high affinity to the N-HR region by the CD analysis. Further, we reveal that SC34EK binds to its target, N-HR in identical manner that C34 does by the structure analysis.

The structural analysis of the N36/SC34EK complex clearly demonstrated that the interaction between SC34EK and N36 peptides was maintained by hydrophobic contacts and that the EK motif was directed toward the solvent. The introduction of the EK residues increased the proportion of accessible surface area occupied by charged residues. Although tight bonding was not observed, a continuous electrostatic potential between the EK residues may serve to stabilize the helix bundle. Such helix stabilization, which might occur on the surface of the HIV-1 virion between SC34EK and the N36 region of gp41, could result in the high anti-HIV-1 activity. In this regard, SC34EK, containing an aligned EK motif, showed more potent anti-HIV-1 activity compared to SC34, which has one misaligned EK motif (Fig. 2a). Increasing the hydrophilic surface area may prevent aggregation of SC34EK as compared to parental peptide C34. Therefore, SC34EK might distribute into the various organs in the body without being trapped and destroyed in the reticular systems or having its activity reduced by non-specific binding to proteins (e.g., albumin) (Fig. 3).

We further demonstrate that SC34EK specifically binds to the target, N-HR of HIV-1, since it only exerted weak activity to two

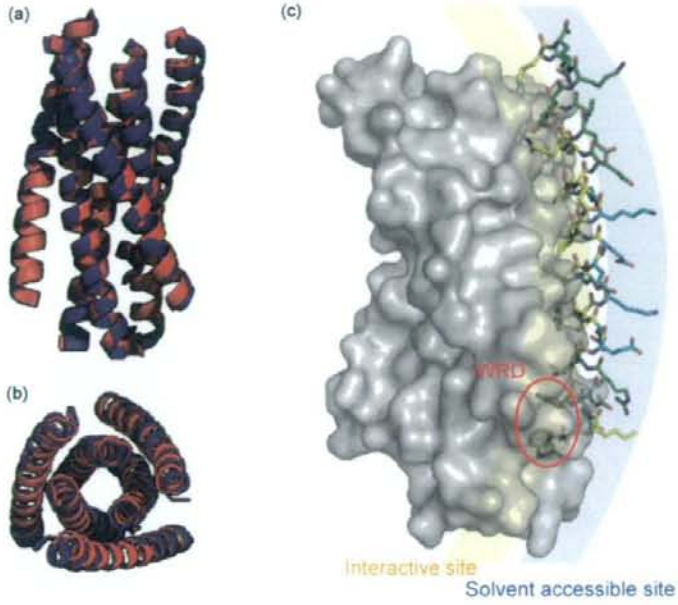

Fig. 5. Structure of the 6-helix bundle formed by N36 and SC34EK. (a and b) The gp41 core structure and N36/SC34EK complex are shown in red and blue, respectively. (c) Stick model representation of SC34EK. The stick model of SC34EK is shown, and three N36s in the core and two other surrounded SC34EK are represented in gray. SC34EK showed amphiphilic properties. The location of the N-terminal tryptophan rich domain (WRD) in SC34EK is indicated by a red circle. Original and introduced charged amino acids are indicated in green and blue, respectively.

HIV-2 strains that contain 15 amino acid substitutions in the N-HR compared to HIV-1 NL4-3 strain (Table 3 and Fig. 2b). These results suggest that to develop resistance to SC34EK, at least, certain mutations in not only the N-HR but also the C-HR are required to be introduced. This might delay emergence of resistant HIV-1 variants to SC34EK in vivo.

So far, some approaches for stabilizing α-helix structures through the introduction of artificial amino acids were reported for HIV-1 fusion inhibitors T-20 (Judice et al., 1997) and C34 (Sia et al., 2002), including an example of an amino acid containing terminal olefin-derived side chains, designed as a substrate for the ring-closing olefin metathesis (Blackwell et al., 2001) and an example of a hydrocarbon-stapled peptides (Phelan et al., 1997) Walensky et al. (2004) applied a hydrocarbon-stapled modification to generate peptides that bind to the BH3 helical domain of Bcl-2, an anti-apoptotic protein, and demonstrated that a synthesized peptide mimic that binds to the BH3 domain activates apoptosis in leukemic cells. However, all peptides exerted only moderate activity in vivo, although they showed efficient binding to the target proteins in vitro (Blackwell et al., 2001; Judice et al., 1997; Sia et al., 2002; Walensky et al., 2004). It is likely that during the formation of the 6-helix bundle and the fusion process, gp41 changes its conformation drastically, suggesting that a flexible conformation of the peptide may be required to preserve actual inhibition. Compared with tethered, constrained peptides, EK modification that facilitates electrostatic stabilization displays such flexibility while exhibiting enhanced α-helicity. Most recently, T290676, a 38 amino acid peptide, has been reported to suppress various fusion inhibitor-resistant strains of HIV-1 (Dwyer et al., 2007). Like SC34EK, T290676 is substituted with the charged and hydrophilic amino acids, glutamic acid (E) and arginine (R), at the solvent accessible site and shows potent anti-HIV-1 activity.

In conclusion, we have demonstrated that SC34EK selectively inhibits various HIV-1 strains, including T-20 resistant clones, through increased stability of the α-helix. The sequence of the solvent accessible site of α-helical peptides is replaceable and modifications of this sequence can regulate α-helicity with target specificity. Therefore, our approach of introducing the EK motif in the α-helical structure of the peptide inhibitor will help to generate future peptide inhibitors with high anti-HIV efficacy and potentially fewer adverse effects.

Acknowledgements

This work was supported in part by grants for the Promotion of AIDS Research from the Ministry of Health and Welfare and for the Ministry of Education, Culture, Sports, Science, and Technology (MEXT) of Japan (E.K. and S.O.); a grant for Research for Health Sciences Focusing on Drug Innovation from the Japan Health Sciences Foundation (E.K., S.O., N.F. and M.M.), the Program of Founding Research Centers for Emerging and Reemerging Infectious Diseases by the MEXT (S.N.), a Health and Labor Sciences Research Grant for Research on HIV/AIDS from the Ministry of Health and Labor of Japan (S.N.), and the 21st Century COE program (H.N., K.K., K.I. and N.F.). H.N. is grateful for the JSPS Research Fellowships for Young Scientists. Appreciation is expressed to Mr. Maxwell Reback (Kyoto University) for reading this manuscript.

References

Aquaro S, D'Arrigo R, Svicher V, Perri GD, Caputo SL, Visco-Comandini U, et al. Specific mutations in HIV-1 gp41 are associated with immunological success in HIV-1-infected patients receiving enfuvirtide treatment. J Antimicrob Chemother 2006;58:714–22.

Armand-Ugon M, Gutierrez A, Clotet B, Este JA. HIV-1 resistance to the gp41-dependent fusion inhibitor C-34. Antiviral Res 2003;59:137–42.

Baba M, Yuasa S, Niwa T, Yamamoto M, Yabuuchi S, Takashima H, et al. Effect of human serum on the in vitro anti-HIV-1 activity of 1-[(2-hydroxyethoxy)methyl]-6-(phenylthio)thymine (HEPT) derivatives as related to their lipophilicity and serum protein binding. Biochem Pharmacol 1993;45:2507–12.
Baldwin CE, Berkhout B. Second site escape of a T20-dependent HIV-1 variant by a single amino acid change in the CD4 binding region of the envelope glycoprotein. Retrovirology 2006;3:84.
Blackwell HE, Sadowsky JD, Howard RJ, Sampson JN, Chao JA, Steinmetz WE, et al. Ring-closing metathesis of olefinic peptides: design, synthesis, and structural characterization of macrocyclic helical peptides. J Org Chem 2001;66:5291–302.
Cabrera C, Marfil S, Garcia E, Martinez-Picado J, Bonjoch A, Bofill M, et al. Genetic evolution of gp41 reveals a highly exclusive relationship between codons 36, 38 and 43 in gp41 under long-term enfuvirtide-containing salvage regimen. AIDS 2006;20:2075–80.
Chan DC, Chutkowski CT, Kim PS. Evidence that a prominent cavity in the coiled coil of HIV type 1 gp41 is an attractive drug target. Proc Natl Acad Sci U S A 1998;95:15613–7.
Chan DC, Fass D, Berger JM, Kim PS. Core structure of gp41 from the HIV envelope glycoprotein. Cell 1997;89:263–73.
Chan DC, Kim PS. HIV entry and its inhibition. Cell 1998;93:681–4.
Derdeyn CA, Decker JM, Sfakianos JN, Wu X, O'Brien WA, Ratner L, et al. Sensitivity of human immunodeficiency virus type 1 to the fusion inhibitor T-20 is modulated by coreceptor specificity defined by the V3 loop of gp120. J Virol 2000;74:8358–67.
Derdeyn CA, Decker JM, Sfakianos JN, Zhang Z, O'Brien WA, Ratner L, et al. Sensitivity of human immunodeficiency virus type 1 to fusion inhibitors targeted to the gp41 first heptad repeat involves distinct regions of gp41 and is consistently modulated by gp120 interactions with the coreceptor. J Virol 2001;75:8605–14.
Dwyer JJ, Wilson KL, Davison DK, Freel SA, Seedorff JE, Wring SA, et al. Design of helical, oligomeric HIV-1 fusion inhibitor peptides with potent activity against enfuvirtide-resistant virus. Proc Natl Acad Sci U S A 2007;104:12772–7.
Ferrer M, Kapoor TM, Strassmaier T, Weissenhorn W, Skehel JJ, Oprian D, et al. Selection of gp41-mediated HIV-1 cell entry inhibitors from biased combinatorial libraries of non-natural binding elements. Nat Struct Biol 1999;6:953–60.
Fikkert V, Cherepanov P, Van Laethem K, Hantson A, Van Remoortel B, Pannecouque C, et al. env chimeric virus technology for evaluating human immunodeficiency virus susceptibility to entry inhibitors. Antimicrob Agents Chemother 2002;46:3954–62.
Foda M, Harada S, Maeda Y. Role of V3 independent domains on a dual-tropic human immunodeficiency virus type 1 (HIV-1) envelope gp120 in CCR5 coreceptor utilization and viral infectivity. Microbiol Immunol 2001;45:521–30.
Judice JK, Tom JY, Huang W, Wrin T, Vennari J, Petropoulos CJ, et al. Inhibition of HIV type 1 infectivity by constrained alpha-helical peptides: implications for the viral fusion mechanism. Proc Natl Acad Sci U S A 1997;94:13426–30.
Kajiwara K, Kodama E, Matsuoka M. A novel colorimetric assay for CXCR4 and CCR5 tropic human immunodeficiency viruses. Antivir Chem Chemother 2006;17:215–23.
Kimpton J, Emerman M. Detection of replication-competent and pseudotyped human immunodeficiency virus with a sensitive cell line on the basis of activation of an integrated beta-galactosidase gene. J Virol 1992;66:2232–9.
Kodama EI, Kohgo S, Kitano K, Machida H, Gatanaga H, Shigeta S, et al. 4′-Ethynyl nucleoside analogs: potent inhibitors of multidrug-resistant human immunodeficiency virus variants in vitro. Antimicrob Agents Chemother 2001;45:1539–46.
Kuiken C, Foly B, Hahn B, Marx P, McCutchan F, Mellors J, et al.Kuiken C, Foly B, Hahn B, Marx P, McCutchan F, Mellors J, Wolinsky S, Korber B, editors. HIV Sequence Compendium 2001. Los Alamos, NM: Los Alamos National Laboratory; 2001.
Lalezari JP, Henry K, O'Hearn M, Montaner JS, Piliero PJ, Trottier B, et al. Enfuvirtide, an HIV-1 fusion inhibitor, for drug-resistant HIV infection in North and South America. N Engl J Med 2003;348:2175–85.
Lazzarin A, Clotet B, Cooper D, Reynes J, Arasteh K, Nelson M, et al. Efficacy of enfuvirtide in patients infected with drug-resistant HIV-1 in Europe and Australia. N Engl J Med 2003;348:2186–95.
Liu S, Lu H, Niu J, Xu Y, Wu S, Jiang S. Different from the HIV fusion inhibitor C34, the anti-HIV drug fuzeon (T-20) inhibits HIV-1 entry by targeting multiple sites in gp41 and gp120. J Biol Chem 2005;280:11259–73.
Maeda Y, Foda M, Matsushita S, Harada S. Involvement of both the V2 and V3 regions of the CCR5-tropic human immunodeficiency virus type 1 envelope in reduced sensitivity to macrophage inflammatory protein 1alpha. J Virol 2000;74:1787–93.
Maeda Y, Venzon DJ, Mitsuya H. Altered drug sensitivity, fitness, and evolution of human immunodeficiency virus type 1 with pol gene mutations conferring multi-dideoxynucleoside resistance. J Infect Dis 1998;177:1207–13.
Marqusee S, Baldwin RL. Helix stabilization by Glu-.Lys+ salt bridges in short peptides of de novo design. Proc Natl Acad Sci U S A 1987;84:8898–902.
Matthews T, Salgo M, Greenberg M, Chung J, DeMasi R, Bolognesi D. Enfuvirtide: the first therapy to inhibit the entry of HIV-1 into host CD4 lymphocyte. Nat Rev Drug Discov 2004;3:215–25.
McRee DE. XtalView/Xfit—a versatile program for manipulating atomic coordinates and electron density. J Struct Biol 1999;125:156–65.
Menzo S, Castagna A, Monachetti A, Hasson H, Danise A, Carini E, et al. Genotype and phenotype patterns of human immunodeficiency virus type 1 resistance to enfuvirtide during long-term treatment. Antimicrob Agents Chemother 2004;48:3253–9.
Mink M, Mosier SM, Janumpalli S, Davison D, Jin L, Melby T, et al. Impact of human immunodeficiency virus type 1 gp41 amino acid substitutions selected during enfuvirtide treatment on gp41 binding and antiviral potency of enfuvirtide in vitro. J Virol 2005;79:12447–54.
Murshudov GN, Vagin AA, Lebedev A, Wilson KS, Dodson EJ. Efficient anisotropic refinement of macromolecular structures using FFT. Acta Crystallogr 1999;D55:247–55.
Nameki D, Kodama E, Ikeuchi M, Mabuchi N, Otaka A, Tamamura H, et al. Mutations conferring resistance to human immunodeficiency virus type 1 fusion inhibitors are restricted by gp41 and Rev-responsive element functions. J Virol 2005;79:764–70.
Navaza J. Implementation of molecular replacement in AMoRe. Acta Crystallogr 2001;D57(Pt 10):1367–72.
Otaka A, Nakamura M, Nameki D, Kodama E, Uchiyama S, Nakamura S, et al. Remodeling of gp41-C34 peptide leads to highly effective inhibitors of the fusion of HIV-1 with target cells. Angew Chem Int Ed Engl 2002;41:2937–40.
Otwinowski Z, Minor W. Processing of X-ray diffraction data collected in oscillation mode. Met Enzymol 1997;276:307–26.
Phelan JC, Skelton NJ, Braisted AC, McDowell RS. A general method for constraining short peptides to an alpha-helical conformation. J Am Chem Soc 1997;119:455–60.
Poveda E, Rodes B, Labernardiere JL, Benito JM, Toro C, Gonzalez-Lahoz J, et al. Evolution of genotypic and phenotypic resistance to Enfuvirtide in HIV-infected patients experiencing prolonged virologic failure. J Med Virol 2004;74:21–8.
Poveda E, Rodes B, Toro C, Martin-Carbonero L, Gonzalez-Lahoz J, Soriano V. Evolution of the gp41 env region in HIV-infected patients receiving T-20, a fusion inhibitor. AIDS 2002;16:1959–61.
Reeves JD, Gallo SA, Ahmad N, Miamidian JL, Harvey PE, Sharron M, et al. Sensitivity of HIV-1 to entry inhibitors correlates with envelope/coreceptor affinity, receptor density, and fusion kinetics. Proc Natl Acad Sci U S A 2002;99:16249–54.
Rimsky LT, Shugars DC, Matthews TJ. Determinants of human immunodeficiency virus type 1 resistance to gp41-derived inhibitory peptides. J Virol 1998;72:986–93.
Salzwedel K, West JT, Hunter E. A conserved tryptophan-rich motif in the membrane-proximal region of the human immunodeficiency virus type 1 gp41 ectodomain is important for Env-mediated fusion and virus infectivity. J Virol 1999;73:2469–80.
Sia SK, Carr PA, Cochran AG, Malashkevich VN, Kim PS. Short constrained peptides that inhibit HIV-1 entry. Proc Natl Acad Sci U S A 2002;99:14664–9.
Walensky LD, Kung AL, Escher I, Malia TJ, Barbuto S, Wright RD, et al. Activation of apoptosis in vivo by a hydrocarbon-stapled BH3 helix. Science 2004;305:1466–70.
Wei X, Decker JM, Liu H, Zhang Z, Arani RB, Kilby JM, et al. Emergence of resistant human immunodeficiency virus type 1 in patients receiving fusion inhibitor (T-20) monotherapy. Antimicrob Agents Chemother 2002;46:1896–905.
Weiner MP, Costa GL, Schoettlin W, Cline J, Mathur E, Bauer JC. Site-directed mutagenesis of double-stranded DNA by the polymerase chain reaction. Gene 1994;151:119–23.
Wild C, Oas T, McDanal C, Bolognesi D, Matthews T. A synthetic peptide inhibitor of human immunodeficiency virus replication: correlation between solution structure and viral inhibition. Proc Natl Acad Sci U S A 1992;89:10537–41.
Xu L, Pozniak A, Wildfire A, Stanfield-Oakley SA, Mosier SM, Ratcliffe D, et al. Emergence and evolution of enfuvirtide resistance following long-term therapy involves heptad repeat 2 mutations within gp41. Antimicrob Agents Chemother 2005;49:1113–9.
Xu Y, Hixon MS, Dawson PE, Janda KD. Development of a FRET assay for monitoring of HIV gp41 core disruption. J Org Chem 2007;72:6700–7.

Statistical Validation of the Relationships of Cancer Pain Relief With Various Factors Using Ordered Logistic Regression Analysis

Yuko Kanbayashi, MPh,†‡ Kousuke Okamoto, PhD,‡ Takanori Ogaru, PhD,‡§ Toyoshi Hosokawa, MD, PhD,* and Tatsuya Takagi, PhD‡‖¶*

Objective: To clarify the relationships of cancer pain with various factors that prevent pain control statistically.

Methods: The participants were 71 terminal cancer patients admitted to the Department of Hematology/Oncology or Department of Gastroenterology/Hepatology, University Hospital, Kyoto Prefectural University of Medicine in whose pain control a pharmacist was involved as part of her clinical duties from January 2004 to November 2006. The effectiveness of pain control was evaluated using a 5-point verbal rating scale (0 = excellent, 1 = good, 2 = moderate, 3 = poor, and 4 = very poor) by interviewing the patients. As pain was rated using a graded scale and as many factors were involved in pain, analysis was performed using ordered logistic regression analysis. Moreover, prediction of an optimal model was performed by leave-one-out cross-validation to eliminate unnecessary variables. A program to perform leave-one-out cross-validation by ordered logistic regression analysis was prepared, independent variables used in the model were increased one by one, and calculation was performed in all combinations. Then, the optimal model was predicted by calculating the percent accuracy of predictions and Spearman rank correlation coefficient.

Results: Nausea [odds ratio (OR) = 1.948, $P = 0.0232$], sex (OR = 2.322, $P = 0.0030$), and bone metastasis (OR = 2.367, $P = 0.0017$) remained as variables significantly correlated with pain when the number of independent variables was 5, and sex (OR = 2.167, $P = 0.006$) and bone metastasis (OR = 2.093, $P = 0.005$) remained when the number of variables was 6.

Discussion: The statistical identification of factors preventing pain control is considered to contribute to the establishment of an evidence-based approach to cancer pain relief.

Key Words: cancer pain, pain relief, palliative care, ordered logistic regression analysis, sex differences

(*Clin J Pain* 2009;25:65–72)

Received for publication November 23, 2007; revised March 11, 2008; accepted April 28, 2008.

From the *Department of the Pain Treatment and Palliative Care Unit; †Department of Hospital Pharmacy, Kyoto Prefectural University of Medicine, Kyoto; ‡Graduate School of Pharmaceutical Sciences; ‖Genome Information Research Center, Research Institute for Microbial Deseases, Osaka University; ¶Research Collaboration Center on Emerging and Re-emerging Infections, Suita; and §Medicinal Chemistry Laboratories, Tanabe Seiyaku Co Ltd, Osaka, Japan.

Reprints: Tatsuya Takagi, PhD, Graduate School of Pharmaceutical Sciences, Osaka University, 1-6 Yamadaoka, Suita, Osaka 565-0871, Japan (e-mail: ttakagi@PHS.osaka-u.ac.jp).

Copyright © 2008 by Lippincott Williams & Wilkins

Both pain treatment and palliative care have been areas farthest from evidence-based medicine (EBM), and many treatments in these fields have been performed on the basis of experience. EBM must also be established in pain relief by performing clinical studies on problems including pain assessment, effective use of drugs, and methods for the management of adverse effects.

Cancer pain is one of the major physical symptoms of cancer patients and the symptom that appears earliest among them, being reportedly observed in 30% to 40% of patients at the diagnosis of cancer and in 65% to 85% of patients with advanced cancer.[1–3] Cancer pain can be palliated by pain relief treatments of the World Health Organization in 85% to 95% of patients,[4–9] but pain control is still insufficient in some patients despite the administration of analgesics at sufficient doses. In the year 2002, the World Health Organization emphasized that "palliative care is an approach that improves the quality of life of patients and their families facing the problem associated with life-threatening illness, through the prevention and relief of suffering by means of early identification and impeccable assessment and treatment of pain and other problems, physical, psychosocial, and spiritual.[10]" In the year 1996, the American Society of Clinical Oncology also declared in the mission statement, "it is the oncologists' responsibility to care for their patients in a continuum that extends from the moment of diagnosis throughout the course of the illness. In addition to appropriate anticancer treatment, this includes symptom control and psychosocial support during all phases of care, including those during the last phase of life.[11]"

Pain is nothing other than the report of "pain" by patients. However, pain is multifaceted, and Twycross[12] observed in his *Symptom Management in Advanced Cancer* that pain is easier to understand when it is regarded as total pain consisting of physical, psychologic, social, and spiritual pain.

We performed this study to clarify the relationships of cancer pain relief with various factors that prevent pain control. The actual procedure used was ordered logistic regression analysis, as pain was evaluated by a graded scale and as multiple factors involved in pain must be evaluated simultaneously.

PATIENTS AND METHODS

Study Term and Participants

The participants were 71 terminal cancer patients admitted to the Department of Hematology/Oncology or Department of Gastroenterology/Hepatology, University Hospital, Kyoto Prefectural University of Medicine from

January 2004 to November 2006 in whose pain control a pharmacist was involved as part of her clinical duties. This study was performed with approval of the Ethical Review Boards of Kyoto Prefectural University of Medicine and Osaka University. Patients with whom no communication was possible throughout the hospitalization period were excluded from the participants. Opioids were administered for the control of cancer pain Table 1 shows the characteristics of the 71 patients.

TABLE 1. Patients Characteristics and Extracted Factors That May Affect Pain When Pain State (After) was Evaluated (n = 71)

	n (0/1)*	Mean ± SD	Range
Sex, female/male	24/47		
Age (y)		65 ± 10	35-84
Infection	33/38		
Previous chemotherapy	7/64		
Married	8/63		
Bone metastasis	45/26		
Outcome	47/24		
Physical symptoms			
Nausea	36/35		
Vomiting	47/24		
Constipation	33/38		
Appetite	67/4		
Dyspnea	48/23		
Cough	48/23		
Fever	29/42		
Psychiatric symptoms			
Depression	47/24		
Delirium	44/27		
Malaise	16/55		
Sleep disorders	46/25		
Confusion	43/28		
Hallucination	4526		
Sleepiness	39/32		
Concomitant medications			
NSAIDs	14/57		
Steroids	39/32		
Analgesic adjuvants	59/12		
Daily dosage of opioid			
Morphine IV mg		16.6 ± 81.6	0-670
Log (morphine IV mg)		−0.18 ± 1.51	−2-2.8
Fentanyl patch μg		3.13 ± 4.7	0-20
Log (fentanyl patch μg)		−0.55 ± 1.34	−2-1.4
Oxycodone p.o. mg		3.8 ± 9.16	0-40
Log (oxycodone p.o. mg)		−1.37 ± 1.29	−2-1.60
Liver function			
AST, U/L		200.1 ± 545	8-4410
ALT, U/L		102.3 ± 230	7-1856
ALP, U/L		903 ± 875	66-4690
γ-GT, U/L		187.6 ± 206.2	12-1018
Bilirubin, mg/dL		6.5 ± 10.5	0.21-38.6
Kidney function			
Serum creatinine, mg/dL		1.42 ± 1.43	0.28-8.54
Other laboratory test items			
Total protein, mg/dL		5.93 ± 1.29	3.3-11.3
Hemoglobin, g/dL		9.13 ± 2.13	3.1-13.3
Platelet, $\times 10^3/\mu L$		176 ± 119	3-468
Type of cancer			
Gastric	10		
Esophageal	10		
Pancreas	17		
Liver	11		
Gall bladder	4		
Cholangiocarcinoma	3		
Lymphoma	7		
Myeloma	2		
Others	7		

*The binary scales were female = 0 and male = 1 for sex, death = 0 and hospital change or discharge = 1 for outcome, and absent = 0 and present = 1 for others.

ALP indicates alkaline phosphatase; ALT, alanine aminotransferase; AST, aspartate aminotransferase; γ-GT, γ-glutamyltransferase; NSAIDs, nonsteroidal anti-inflammatory drugs; P.O., peros.

Evaluation of the State of Pain

Three kinds of the states of pain were evaluated by interviewing the patients using a 5-point verbal rating scale (VRS; 0 = excellent, 1 = good, 2 = moderate, 3 = poor, and 4 = very poor).

The dependent variable (Y = after) was defined as the state of pain just before hospital discharge or the last opportunity of communication. The dependent variable (Y = before) was defined as the state of pain on admission when pain control was poorest. The dependent variable (Y = before-after), improvement factor.

Statistical Analysis

Extraction of Variables

Variables were extracted in preparation for the analysis of multiple factors concerning pain control by regression analysis. The rating of pain on the VRS (Y = after) was 0 in 28 patients, 1 in 29, 2 in 11, 3 in 3, and 4 in none; the rating of pain on the VRS (Y = before) was 0 in 0 patients, 1 in 2, 2 in 12, 3 in 24, and 4 in 33; and improvement factor (Y = before-after) was 0 in 0 patients, 1 in 8, 2 in 31, 3 in 28, and 4 in 4 (Table 2).

The minimum number of patients necessary to form a category of the dependent variable was 4 in the ordered logistic regression analysis used in this study and fewer patients were rated as 3 or 4 (Y = after). Therefore, Y = after was recategorized into 3 levels: new level 0 indicates the original levels 0, new level 1 indicates the original levels 1, and new level 2 indicates the original levels 2, 3, and 4 (Table 3). Similarly, improvement factor (Y = before-after) was recategorized into 3 levels: new level 1 indicates the original levels 0 and 1, new level 2 indicates the original levels 2, and new level 3 indicates the original levels 3 and 4 (Table 4).

© 2008 Lippincott Williams & Wilkins

TABLE 2. The Rating of Pain on the VRS (After, Before) and Improvement Factor (n = 71)

VRS	After Male (Female)	Before (Male, Female)	Improvement Factor (Male, Female)
0	28 (14)	0	0
1	29 (20)	2 (1)	8 (7)
2	11 (10)	12 (9)	31 (23)
3	3 (3)	24 (12)	28 (15)
4	0	33 (25)	4 (2)

VRS indicates verbal rating scale.

Table 1 shows the independent variables (X) extracted from clinical records (retrospective survey). Binary scales were female = 0 and male = 1 for sex, death = 0 and hospital change/discharge = 1 for outcome, and no = 0 and yes = 1 for other factors.

Analytical Procedure

Ordered Logistic Regression Analysis (JMP 6: SAS Institute)

Ordered logistic regression analysis examines whether changes in variable Y (dependent variable) can be explained by changes in m variables (X_1, X_2,..., X_m) (independent variables). For example, changes in the dependent variable Y are represented by the model: $Y = b_0 + b_1X_1 + b_2X_2 + \ldots + b_mX_m$ in multiple regression analysis and by the model: $\log\{Y/(1\text{-}Y)\} = b_0 + b_1X_1 + b_2X_2 + \ldots + b_mX_m$ in logistic regression analysis. In these models, b_0 is a constant member in the equation and b_1, b_2,..., b_m, which represent the relationship between Y and X_i after elimination of the effects among the independent variables, are called partial regression coefficients. Regression analysis allows prediction concerning unknown data by constructing a model representing the phenomenon defined as the dependent variable on the basis of available data. Also, by evaluating the degree of the effect of each independent variable on the dependent variable according to the partial regression coefficient, it allows the analysis of factors (independent variables) that affect the dependent variable. In multiple regression analysis, dependent variables are continuous data, such as the concentration of a substance in blood, that are assumed to be linearly related to the independent variable. This concept of multiple regression can also be used to simultaneously examine the relationships among 2 or more categorical variables. However, the relationships among categorical variables are not simply linear, because the ranges of their values are finite. Therefore, generalized linear models are used. If quantitative variables are included in independent variables, and if the dependent variable is a categorical variable, logistic regression analysis can be performed by applying a generalized linear model through converting the probability that the value of a categorical variable falls in a particular category (p) into log {p/(1-p)}, which can take infinitely small to infinitely large values (logit conversion). A logistic regression analysis can be used for binary variables such as pain (present or absent). If there are 3 or more categorical variables in this study, ordered logistic regression analysis can be used. Ordered logistical regression analysis was performed in this study to efficiently use the variables (Y = after, before, or improvement factor) extracted by means of a 5-point scale and because a large number of factors (X in Table 1) are involved in pain.

TABLE 3. Dependent Variable (Y = After): Categorization of Data

Dependent Variable (Y)	VRS	No. Patients (71)
0	0	28
1	1	29
2	2, 3, 4	14

VRS indicates verbal rating scale.

TABLE 4. Dependent Variable (Y = Improvement Factor): Categorization of Data

Dependent Variable (Y)	Before-After	No. Patients (71)
1	0, 1	8
2	2	31
3	3, 4	32

Leave-one-out Cross-validation (LOOCV)

The ultimate objective of many multivariate analysis procedures is to construct a model for the prediction of related factors. In regression analysis, the relationships between the quantitative properties of samples of a variable (dependent variable) with those of 1 or more independent variables are established as a model. A common phenomenon that requires caution in all regression analysis procedures is that if the number of variables simultaneously considered in the model (m) is excessively large, results that "overfit" the data may be obtained to reduce the predictive ability of the model. Also, if the number of samples of each variable is insufficient, the reliability of the model is impaired. Usually, the necessary number of samples (n) is reported to be 5 to 10 times the number of variables (m). After the construction of a model by applying multivariate analysis, the appropriateness of the model must be confirmed by checking, for example, whether overfitting, which was described above, has occurred.

Overfitting is a loss in the applicability of the model to data other than training data (data used for the preparation of a model) owing to overadjustment of the estimated values of the parameter to training data in the learning process of a categorization model using many parameters. To avoid overfitting, parameters must be selected using cross-validation, according to the precision of categorization of the test data prepared for the measurement of the predictive ability using data other than the training data.

Cross-validation means dividing data into 2 parts, preparing a model using one of them as training data, and examining the predictive ability of the model using the other part as test data. It is a technique to evaluate the number of variables used and predictive ability of the model equation itself. The procedure of LOOCV used in this study was as follows. First, 1 sample is temporarily excluded from the training data and a model is constructed

© 2008 Lippincott Williams & Wilkins

using the remaining training data. By employing this model, the dependent variable of the excluded sample is predicted, and the difference between the actual and predicted values of the dependent variable is recorded. Thereafter, the excluded sample is returned to the training data, another sample is excluded, a new model is constructed, and a new predicted value and its difference compared with the actual value are obtained. This process is repeated until all samples have been excluded once each. The optimal model can, thus, be selected from multiple models by comparison of the predictive ability.

Statistics and criteria used for this comparison are described as follows.

1. The percent accuracies of the model using test data by LOOCV.
2. Spearman rank correlation coefficients calculated according to the following expressions.

$$(R^2) = 1 - \frac{6\sum d^2}{n^3 - n}$$

d = the difference between each rank of corresponding values of x (= observed value) and y (= the predicted value), and n = the number of pairs of values.

RESULTS

Course of Analysis and Results

First, to accurately preserve the model, independent variables unnecessary for expressing the data as a model were excluded by calculating the percent accuracy. Independent variables were further screened by examining the multicolinearity, which occurs when there are correlations among independent variables and leads to the preparation of inappropriate models. As a result, 23 independent variables could be selected (Table 5) and the accuracy was 53/71.

Independent variables were further eliminated by estimating the optimal model on the basis of the evaluation of the predictive ability by LOOCV. A program to perform LOOCV by ordered logistic regression analysis was coded by us, and the optimal model was predicted by calculating the percent accuracy of the prediction results and Spearman rank correlation coefficients between the actual dependent variable and prediction results.

In the process of reducing independent variables one at a time from the 23, the calculation program stopped when all variables had been applied. Therefore, we divided the 23 independent variables into 4 categories consisting of 6, 6, 6, and 5 variables and further eliminated them. The 4 categories were established by combining independent variables considered to be most closely interrelated and distributing independent variables considered to affect pain control among these categories markedly.[12] For example, category A includes characteristics of patients (eg, sex), B includes physical factors (eg, nausea), C includes psychosocial factors (eg, depression), and D includes laboratory test values (eg, bilirubin). Eliminated independent variables varied according to how they were categorized and the results were unreliable. Therefore, we decided to extract necessary independent variables rather than eliminate unnecessary ones. The predictive ability was calculated first in all models in which only 1 variable was used and by adding 1 variable to the models in all possible combinations. As a result, independent variables that always remained (sex, bone metastasis, and nausea) could be determined when the number of independent variables used in the models was increased to 3-6. The results are shown below.

Procedure 1 [Y=After, Selection of Variables (X) When the Number of Variables was Increased to 5]

Among the combinations of 5 independent variables that gave the highest accuracy (41/71), Spearman rank correlation coefficient was highest (0.516) for the combination of sex, bone metastasis, nausea, sleep disorders, and cough. Ordered logistic regression analysis was performed using these independent variables. As a result, nausea, sex, and bone metastasis were significant (Table 6).

Spearman rank correlation coefficient was highest (0.538) for 8 combinations, all of which included sex, bone

TABLE 5. 23 Independent Variables that Remained After Elimination

Scale of Variable	Selected (23 Variables)	Eliminated (15 Variables)
Binary	Previous chemotherapy, sex, marriage, bone metastasis, outcome	Infection
	Physical symptoms: nausea, appetite, cough, fever	Physical symptoms: nausea, constipation, dyspnea
	Psychiatric symptoms: depression, sleep disorders, sleepiness	Psychiatric symptoms: delirium, malaise, confusion, and hallucination
	Concomitant medications: NSAIDs, steroids, analgesic adjuvants	
Continuous	Age	Opioid: daily dosage of morphine, fentanyl and oxycodone, log (daily dosage of morphine)
	Opioid: log (daily dosage of fentanyl and oxycodone)	Liver function: AST, ALP, γ-GT
	Liver function: ALT, bilirubin	Other laboratory test items: platelet
	Kidney function: Serum creatinine	
	Other laboratory test items: total protein, hemoglobin	

ALP indicates alkaline phosphatase; ALT, alanine aminotransferase; AST, aspartate aminotransferase; γ-GT, γ-glutamyltransferase; NSAIDs, nonsteroidal anti-inflammatory drugs.

© 2008 Lippincott Williams & Wilkins

TABLE 6. Result of Procedure 1-1 (Y=After, Selected Variables When the Number of Variables was Increased to 5 on the Basis of the Percent Accuracy (Accuracy: 41/71, Spearman Rank Correlation Coefficient: 0.516)

Item	Estimated Value	Standard Error	χ^2Value	P	Odds Ratio	Confidence Interval of Odds Ratio	
						Lower 95%	Upper 95%
Sex	0.749	0.273	7.491	0.0061*	2.116	1.262	3.691
Bone metastasis	0.787	0.267	8.678	0.0032*	2.198	1.314	3.797
Nausea	0.553	0.259	4.561	0.0326*	1.738	1.054	2.947
Sleep disorders	0.297	0.262	1.284	0.2571	1.346	0.806	2.259
Cough	−0.123	0.273	0.204	0.6507	0.883	0.510	1.498

*$P < 0.05$.

metastasis, and nausea (total protein, fever, depression, cough, sleepiness, nonsteroidal anti-inflammatory drugs, and steroids were also included in some of them), and the accuracy was 39/71. As a result of ordered logistic regression analysis using these independent variables, nausea, sex, and bone metastasis were also significant (Table 7).

Procedure 2 [Y=After, Selection of Variables (X) When the Number of Variables was Increased to 6]

Spearman's rank correlation coefficient was highest (0.545) for the combination consisting of sex, bone metastasis, nausea, alkaline phosphatase, outcome, constipation, and appetite, and the accuracy was 39/71. Ordered logistic regression analysis was performed using these independent variables. As a result, sex and bone metastasis were significant (Table 8).

Procedure 3 (Y=Improvement Factor)

Improvement factor (Y = before-after) was also evaluated. Similarly to the process performed when the final state of pain (Y = after) was selected as the dependent variable, the percent accuracy and multicolinearity were examined and variables were eliminated by LOOCV. As a result, sex, nausea, steroids, and log (daily dosage of morphine) (accuracy, 40/71; Spearman rank correlation coefficient, 0.328) were selected when the number of variables was increased to 4. When ordered logistic regression analysis was performed using these variables as independent variables, only sex was significant (Table 9).

DISCUSSION

The result of ordered logistic regression analysis revealed cancer pain to be significantly correlated with nausea, sex, and bone metastasis. As shown in Tables 6 to 8, the odds ratio (OR) indicated that pain is exacerbated when the patient is male and has nausea and bone metastasis. The data distribution of these 3 independent variables was 47:24 (male:female) for sex, 35:36 (present:absent) for nausea, and 26:45 (present:absent) for bone metastasis, showing no marked disparity between the categories.

Bone metastasis was significantly correlated with cancer pain. There has been no previous study in which the relationship between bone metastasis and cancer pain was statistically analyzed, but bone metastasis is widely perceived in palliative medicine as the greatest factor that impairs the quality of life.[13–15] External irradiation is a standard pain control treatment for bone metastasis, but internal radiotherapy is also considered in patients with multiple bone metastases to reduce their burden.[16–19] Recently, a report that bisphosphonate is also effective for pain relief has attracted attention, but the evidence is

TABLE 7. Result of Procedure 1-2 (Y=After, Selected Variables When the Number of Variables was Increased to 5 on the Basis of Spearman Rank Correlation Coefficient (Accuracy: 39/71, Spearman Rank Correlation Coefficient: 0.538)

Item	Estimated Value	Standard Error	χ^2Value	P	Odds Ratio	Confidence Interval of Odds Ratio	
						Lower 95%	Upper 95%
Sex	0.842	0.283	8.805	0.0030*	2.322	1.367	4.144
Bone metastasis	0.861	0.275	9.769	0.0017*	2.367	1.392	4.187
Nausea	0.666	0.293	5.147	0.0232*	1.948	1.088	3.615
Total protein	−0.026	0.051	0.255	0.6129	0.974	0.886	1.081
Fever	0.107	0.318	0.112	0.7372	1.112	0.589	2.102
Depression	−0.232	0.301	0.595	0.4401	0.792	0.425	1.443
Cough	−0.125	0.329	0.145	0.7027	0.881	0.446	1.699
Sleepiness	0.076	0.283	0.072	0.7875	1.079	0.617	1.882
NSAIDs	0.012	0.322	0.001	0.9679	1.013	0.522	2.013
Steroids	0.040	0.256	0.024	0.8752	1.041	0.624	1.738

*$P < 0.05$.

NSAIDs indicates nonsteroidal anti-inflammatory drugs.

© 2008 Lippincott Williams & Wilkins